scientific reports

Check for updates

OPEN

An in vitro evaluation of the mineralization effect of a marine collagen supplement on early enamel lesions

Halah Judran Chlaibawi & Lamis A. Al-Taee✉

The marine collagens are biocompatible and biodegradable materials that are considered as a biomimetic approach for tissue regeneration. This study evaluated the effect of daily consumption of marine collagen supplement drink on enamel white spot lesions (WSLs), comparing the results against Regenerate system and Sylc air abrasion methods. Fifty human enamel slabs were allocated into five groups ($n = 10$ per group): non-treated (sound); non-treated (WSLs, 8% methylcellulose gel with 0.1 M lactic acid (pH 4.6) at 37 °C for 21 days); and three treated surfaces with marine collagen; Regenerate system; and Sylc air abrasion. The treatment lasted for 28 days followed by four weeks' storage in artificial saliva (pH = 7.0, 37 °C). Evaluations were conducted via micro-Raman Spectroscopy and Knoop microhardness at varying depths (50–200 µm), followed by morphological assessments using scanning electron microscopy (SEM). The marine collagen-treated surfaces demonstrated higher phosphate intensity and Knoop hardness values (KHN) compared to WSLs ($p < 0.001$) up to 150 µm depth, approaching that of sound enamel and other treated surfaces ($p > 0.05$). A significant positive correlation ($p > 0.001$) was recognized between the mineral content and corresponding KHN, particularly in the superficial layers. Notably, a compact layer of mineral-like structure was observed at the marine-treated surfaces covering the exposed lesion and enhancing surface integrity. These findings suggest that the use of marine collagen supplements can effectively enhance the mineral content and surface integrity of demineralized enamel surfaces up to a depth of 150 µm, presenting significant implications for dental health management.

Tooth enamel is unable to self-regenerate when subjected to significant mineral loss due to dental caries or erosion[1]. Many approaches have been implemented to manage white spot lesions (WSLs), including the use of fluoride[2] microabrasion[3] resin infiltration[2,3] sealants[4] and bioactive materials[5,6] that increase the availability of calcium, phosphate and fluoride ions. These ions are essential for the formation of mineral deposits that restore the structure of demineralized enamel and prevent further mineral loss. Despite the reported effectiveness of these approaches, achieving a pathway for natural tissue repair continues to pose challenges for dental researchers. This method aims to mimic the natural process of remineralization by utilizing protein-based substrates as a biomimetic scaffold, which encourages the development of enamel-like apatite via the presence of saliva. This, in turn, enhances the structural and mechanical properties of demineralized tooth surfaces[7,8].

Collagens are biocompatible and biodegradable compounds that promote cellular adhesion, proliferation, and differentiation by creating an extracellular matrix, that mimics the natural environment, which is crucial for tissue engineering and bone reconstruction[9]. Previous investigations[8–10] highlighted the capability of self-assembling peptides to organize into higher-order structures that mimic the enamel matrix, which aids in tissue regeneration and remineralization. These peptides induce the formation of new mineral structures that are structurally similar to natural enamel while meeting the desired biological requirements.

Marine-derived collagens serve as a potent substitute for animal collagens, free from religious constraints and animal pathogens[11]. They are biocompatible[12] with a reduced immune response[13] higher solubility in water[14] and lower production costs[11]. It has been reported[15] that the marine collagen can induce the remineralization potential and osteogenic differentiation in bone tissue, providing significant benefits for tissue engineering applications.

Regenerate System is a toothpaste with a serum comprising of calcium, silicate, sodium phosphate, and fluoride. The calcium silicate can be transformed into hydroxyapatite, which then precipitates on the

Department of Conservative and Aesthetic Dentistry, Baghdad College of Dentistry, University of Baghdad, Baghdad, Iraq. ✉email: lamis.al-taee@codental.uobaghdad.edu.iq; lamisnaji76@gmail.com

demineralized enamel surfaces[16]. It has been found[17] that the daily application of this system for two weeks can enhance the mineral content and tissue hardness of enamel, promote the formation of mineral-like deposits on the surface, and thereby improve the resistance to acid challenges.

Sylc AquaCare air abrasion represents a non-invasive treatment modality for managing enamel white spot lesions (WSLs). Air abrasion is utilized with a special handpiece that directs a stream of high-speed, fine abrasive particles to remove the superficial layers of demineralized enamel. This process facilitates remineralization and enhances the appearance of WSLs. The powder used is composed of calcium sodium phosphosilicate (bioactive glass particles, 45S5), which can form a hydroxycarbonate apatite (HCA) layer upon contact with saliva. This process creates a calcium- and phosphate-rich layer on the demineralized surfaces, enhancing the structural integrity and mechanical properties of the treated enamel[18–20].

Micro-Raman Spectroscopy serves as a non-invasive tool capable of quantitatively assessing the mineral distribution within dental hard tissues by detecting their specific molecular vibrational signatures[21]. The non-invasive nature of this method facilitates the correlation between mineral content and tissue hardness at designated scanned points. The microhardness test serves as an indicator of the mechanical resilience of dental hard tissues, and can reflect the amount of mineral gain or loss[17].

Upon reviewing the existing literature, it has been found that no previous studies addressed the efficacy of marine collagen in repairing demineralized enamel surfaces. Therefore, this study aimed to evaluate the mineralization effect of marine collagen supplement on enamel white spot lesions (WSLs) in comparison to Regenerate paste *and serum* and Sylc air abrasion. The assessment was carried on via using micro-Raman spectroscopy and Knoop microhardness, through the entire depth of WSLs (50–200 µm), combined with scanning electron microscopy (SEM). The null hypothesis of this study was that there is no significant remineralization effect among the marine collagen supplement, the Regenerate system, Sylc air abrasion, and non-treated surfaces (both sound and WSLs) at different layers of subsurface enamel lesions. Additionally, there was no correlation between mineral content and microhardness at each layer.

Methods

Materials

The materials that were used in this study are presented in Table 1.

Characterization of marine collagen powder with fourier transform-infrared spectroscopy (FT-IR)

Attenuated Total Reflection Fourier Transform Infrared spectroscopy (ATR-FTIR) analysis was performed using IR Affinity-1 S (SHI MADZU, Japan) with 1 cm^{-1} resolution, LabSolutions CS control software was used for data analysis. The infrared spectrum of marine collagen was measured in the spectral range of 400–4000 cm^{-1}, with eight scans each, ($n = 3$).

Specimen Preparation

Ten caries-free human premolars extracted for orthodontic purposes were ethically approved by the health research committee (Ref No. 954, 23/10/2024) and stored in a de-ionized water in a cold cabinet (+4℃). The roots were removed by using a water-cooled diamond blade (330-CA/RS-70300, Struers, Cleveland, USA) at the Cemento-Enamel Junction (CEJ), while the crowns were bisected mesiodistally (Isomet 1000, Buehler, Lake Bluff, IL, USA). Five slabs (3.5 mm height, 3.5 mm width, and 2.0 mm thickness) were obtained from the buccal half of each crown, which were randomly assigned for each group, and then embedded in epoxy resin molds. The specimens ($n = 50$) were then divided into five groups ($n = 10$ per group): Sound (non-treated), WSLs (non-treated), Marine (WSLs immersed in a marine collagen supplement drink), Regenerate (WSLs treated with Regenerate toothpaste/serum), and Sylc (WSLs subjected to Sylc air abrasion), with all groups stored in artificial saliva (pH = 7) for 28 days at 37℃.

The commercial name	Company/country	Lot no	Composition
Premium Marine collagen supplement drink	Nutrabytes, Sweden	CPF050224A	10,000 mg of type 1 & 3 Wild Caught Fish Hydrolysed pure peptides, (pH = 5.0- 7.5)
REGENERATE Enamel Science™ toothpaste/serum	Regenerate NR5 company, France	Toothpaste: 22028CA Serum: 20949CY A	The toothpaste and the serum contain the same ingredients: Glycerin, Calcium Silicate, PEG-8, Trisodium Phosphate, Sodium Phosphate, Aqua, PEG-60, Sodium Lauryl Sulfate, Sodium Monofluorophosphate, Aroma, Hydrated Silica, Synthetic Fluorphlogopite, Sodium Saccharin, Polyacrylic Acid, Tin Oxide, and Limonene, while the activator gel contains Aqua, Glycerin, Cellulose Gum, Sodium Fluoride, Benzyl Alcohol, Ethylhexylglycerin, Phenoxyethanol, Sodium Fluoride (1450 ppm F), (pH = 7–8)
Sylc® bioactive glass	Denfotex Research Ltd, Inverkeithing, UK	359684-27-8	The powder is composed of 100% bioactive glass, which is a calcium sodium phosphor-silicate with particle size ranging from 25 to 120 µm, the ingredients are: silicon 21%, calcium 18%, sodium 18%, phosphorus 3%, oxygen 40%, (pH = 7–10)
Artificial Saliva	Albasheer Scientific Bureau, Iraq		1.5 mM $CaCl_2 \times 2H_2O$; 0.9 mM KH_2PO_4, 130.0 mM KCl; 20.0 mM HEPES, 3.1 mM NaN_3, adjusted to pH 7.0 with KOH[22]
Methylcellulose	Sigma-Aldrich, USA	9004-67-5	MC viscosity 20–30%
Lactic acid	AnalaR, UK	50-21-5	88.0–92.0% DL-Lactic acid, 0.1 mol/L, pH of the was adjusted to 4.60 using 1 M NaOH

Table 1. The materials that were used in this study.

Artificially induced enamel white spot lesions (WSLs)

WSLs were induced following bi-layer demineralization protocol (8% methylcellulose gel buffered with a lactic acid layer (0.1 M, pH 4.6) for 21 days at 37°C[6,18]. Initially, the enamel surfaces received a sequential polishing (Laryee Technology CO.LTD, China) using silicon carbide paper (Versocit, Struers A/S, Copenhagen, Denmark) in a sequential pattern (500-grit silica carbide disk for 5 s, 1200- grit for 10 s, 2000-grit for 30 s and 4000-grit for 2 min). This was followed by 1 min ultrasonication after each step and 4 min after the 4000-grit to remove the smear layer. The methylcellulose powder was mixed with deionized water (100℃) and stirred for 24 h at ambient temperature. Enamel slabs were placed in the bottom of 2 L glass beaker, followed by pouring 800 mL MC gel over the samples, a filter paper was placed on the top of the gel that was kept in the fridge at 4 °C overnight. Then, 800 mL of lactic acid placed over the filter paper, and the pH of lactic acid was adjusted to 4.6 by using 1 M of NaOH, then stored in incubator at 37℃ for 21 days. The solution was refreshed on weekly basis.

Application of marine collagen supplement drink

The solution was prepared following the manufacture instructions by mixing two spoons of Marine collagen powder with 200 ml of distilled water using magnetic stirrer. Then specimens were immersed in the solution for 2 min, to allow the diffusion and self-assembling of collagen on WSLs. The treatment continued once a day for 28 days, followed by four weeks' storage in artificial saliva(pH = 7) at 37℃[23].

The application of regenerate enamel science system

Initially, the WSLs were received frequent application of Regenerate serum for three consecutive days following the manufacturers' instructions. In which the serum and activator were mixed by a magnetic stirrer and applied for three minutes using a disposable brush. This was followed by the application of the toothpaste for 2 min, in which 4 ml of toothpaste was dispensed per specimen and mixed with distilled water using 1:3 dilution ratio, for 4 min until being homogenous[17,23]. Treated specimens were stored in artificial saliva(pH = 7) at 37℃ for 28 days.

Sylc air abrasion (Denfotex research ltd, UK)

An air abrasion handpiece (AquaCare, VELOPEX International, Air Abrasion Unit, 40–46 psi air pressure, 90° nozzle angle, and 5 mm surface distance, circular movement) was used to propel the Sylc powder on WSLs' surfaces following the manufacturer's recommendations[19,20]. Each specimen was treated for 10 s, and the powder was left on the surface for 2 min, followed by washing under running water. A daily application was carried on up to 28 days, followed four weeks' storage in artificial saliva (pH = 7) at 37℃, which was refreshed in daily basis.

micro-Raman spectroscopy

Two hundred scanning were performed over fifty slabs ($n = 4$ per slab) using confocal laser Raman spectroscopy operating in line-scan mode (Senterra, Bruker Optics, Germany, 780 nm near-infrared diode laser, 400 line/mm diffraction grating). The measurements were done throughout the entire depth of lesions (50–200 µm, Fig. 1) with 200–3600 cm^{-1} spectra range (100 mW power, and 30 s integration time). Raman software (OPUS, Bruker Optics, Germany, https://www.bruker.com/en/products-and-solutions/infrared-and-raman/opus spectroscopy-software.html) was used for processing and spectra analysis, and the intensity of the phosphate peaks ν_1 at 960 cm^{-1} (symmetric P-O stretching vibrational mode) was measured[24].

Cross-sectional microhardness

The hardness profile was performed by using HST-1000 Knoop microhardness tester (Jinan Hensgrand Instrument Co, Ltd, China). Two hundred indentations (Four measurements per slab) were made by a Knoop diamond with 25 gf load for 10 s across the lesion depth (50–200 µm, Fig. 1) on the same points that were scanned by micro-Raman spectroscopy[25]. The Knoop hardness number (KHN) was calculated automatically by the manufacturer's software.

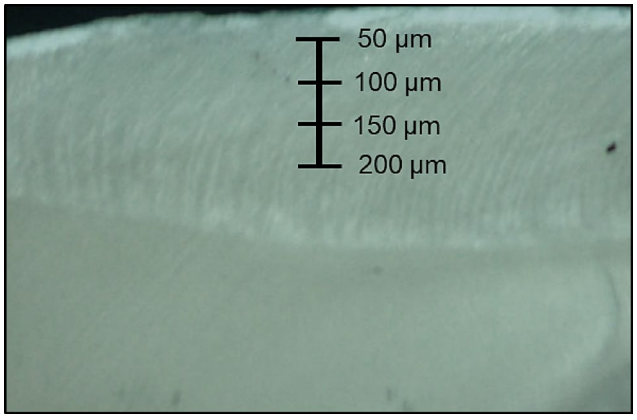

Fig. 1. A representative enamel slab illustrates the points that were analyzed by confocal Raman microspectroscopy, followed by Knoop microhardness (Digital light microscope A. Krüss Optronic Gmbh, Germany magnification power = 20X).

Scanning electron microscope (SEM)

Two representative specimens from each group were gold-coated and viewed under scanning electron microscope (Inspect F50, FEI Company, Eindhoven, The Netherlands) by applying 30 kV accelerating voltage and two magnification powers for the surface view (5000x and 10000x), and 1300x and 5000x for the cross-sectional view.

Statistical analysis

The sample size was calculated by using G-Power 3.0.10 software, developed by Franz-Faul, University of Kiel, Germany, (https://www.psychologie.hhu.de/fileadmin/redaktion/Fakultaeten/Mathematisch-Naturwissenschaftliche_Fakultaet/Psychologie/AAP/gpower/GPowerWin_3.1.9.7.zip)[26]. Given a research power of 90%, an alpha error probability of 0.05 (two-sided), and an effect size of F = 0.25 (medium effect size) was determined for five groups. The required sample size is 50 ($n = 10$ per group, 400 measured points)[17,27,28].

The statistical analyses were conducted using SPSS software version 26.0 (SPSS, Inc., an IBM Company, Chicago, IL, USA, https://www.ibm.com/sps). The equality of variances and normal distribution of the data were tested by using the Shapiro-Wilk test. Since all data showed equal variances and normal distribution, Multivariant ANOVA followed by Tukey's post-hoc multiple comparisons tests were used to analyze the Raman phosphate peak intensity (A.U.) and Knoop microhardness number (KHN) between groups at each layer and between layers ($p < 0.05$). Pearson's correlation coefficient test was used to explore if there was a correlation between Raman phosphate intensity and their equivalent KHN at each layer.

Ethical approval

The study received ethical approval from the Research Ethical Committee (Reference No. 954, 23/10/2024). The authors confirm that informed consent forms for all extracted teeth were obtained from all patients and/or their legal guardians. All procedures were conducted in accordance with the guidelines of the local institutional committee, adhering to the principles of the 1964 Helsinki Declaration and its subsequent amendments, or comparable ethical standards. Ethical considerations were diligently upheld throughout the research process. Specifically, the authors confirm that: (1) No participants were subjected to any potential harm effect from any aspects of the study, (2) The investigation did not include live plants or cytotoxic materials, (3) The materials used during the research were handled in ways that did not pose direct or indirect risks to the researchers or those conducting various measurements, (4) All tools utilized in the study were handled with scientific rigor, ensuring the safety of individuals and conformity with local regulations.

Clinical relevance

Marine collagen derived from the skin and scales of fish has gained popularity as a dietary supplement, particularly the drink form. It is considered more sustainable compared to bovine collagen, and it provides the essential amino acids that can maintain bone density and strength and help in bone repair. This study supported the effectiveness of daily consumption of Marine collagen supplement drink for 28 days to treat WSLs, since it enhanced the chemical, mechanical and morphological characteristics of demineralized enamel surfaces up 150 µm depth in a similar way to another remineralizing approaches.

Results

FT-IR spectral analysis

The FTIR spectra of marine collagen powder confirms the presence amide I, amide II and amide III bands at 1636–1661 cm^{-1}, 1549–1558 cm^{-1} and 1200–1300 cm^{-1}, respectively[29]. The protein band occurring close to 1450 cm^{-1} is assigned to the C-H bending modes and amide-A band (NH stretching), was observed at 3400 cm^{-1}, Fig. 2.

Chemical analysis (micro-Raman Spectroscopy)

All treated and non-treated enamel surfaces showed the evidence of the characteristic phosphate peak ν_1 at 960 cm^{-1} (symmetric P-O stretching vibrational mode) which is the strongest peak in the spectrum. In all groups, there was a gradual increase in the phosphate peak intensity from the outermost layer (50 µm) towards the deepest layer (200 µm), however, this was statistically significant in the WSLs only between the outer layers (50 and 100 µm) and the deeper layers (150 and 200 µm), $p <= 0.001$ and 0.007, respectively).

The demineralized surfaces (WSLs) exhibited a statistically significant reduction in the phosphate peak intensity ($p < 0.001$) in comparison to all groups up to 150 µm. Beyond that depth (200 µm), the difference was statistically not significant from all groups ($p > 0.05$). By comparing the phosphate intensity between treated enamel surfaces (Marine, Regenerate, and Sylc), the difference was statistically not significant throughout the lesion depth (50–200 µm). Although, the intensity values in all treated surfaces were higher than sound throughout the lesion depth, but the difference was statistically not significant ($p > 0.05$), (Fig. 3).

Cross-sectional microhardness

There was a gradual increase in KHN values from the superficial layer (50 µm) towards the deeper layers in all groups, however, this raise was only statistically significant in the WSLs groups at 200 µm ($p < 0.001$). All treated surfaces (Marine, Regenerate, and Sylc) recorded statistically significantly higher KHN than WSLs ($p < 0.001$) up to 150 µm, however, at 200 µm, the difference was statistically not significant between groups ($p > 0.05$). All treated surfaces showed comparable KHN throughout the entire depth of the lesions ($p > 0.05$). Although the values in all treated groups were higher than the sound surfaces, but statistically, the difference was not significant ($p > 0.05$), Fig. 4.

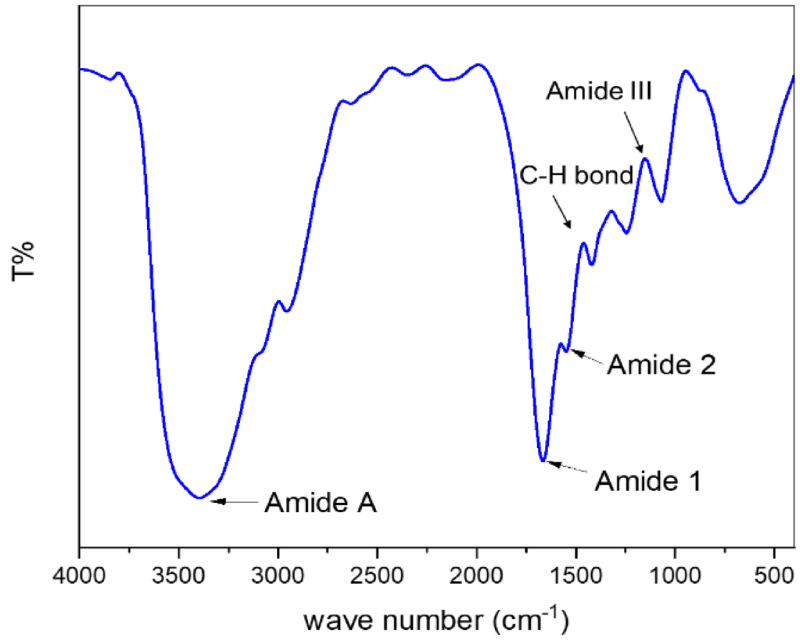

Fig. 2. FT-IR spectrum of the Marine collagen powder.

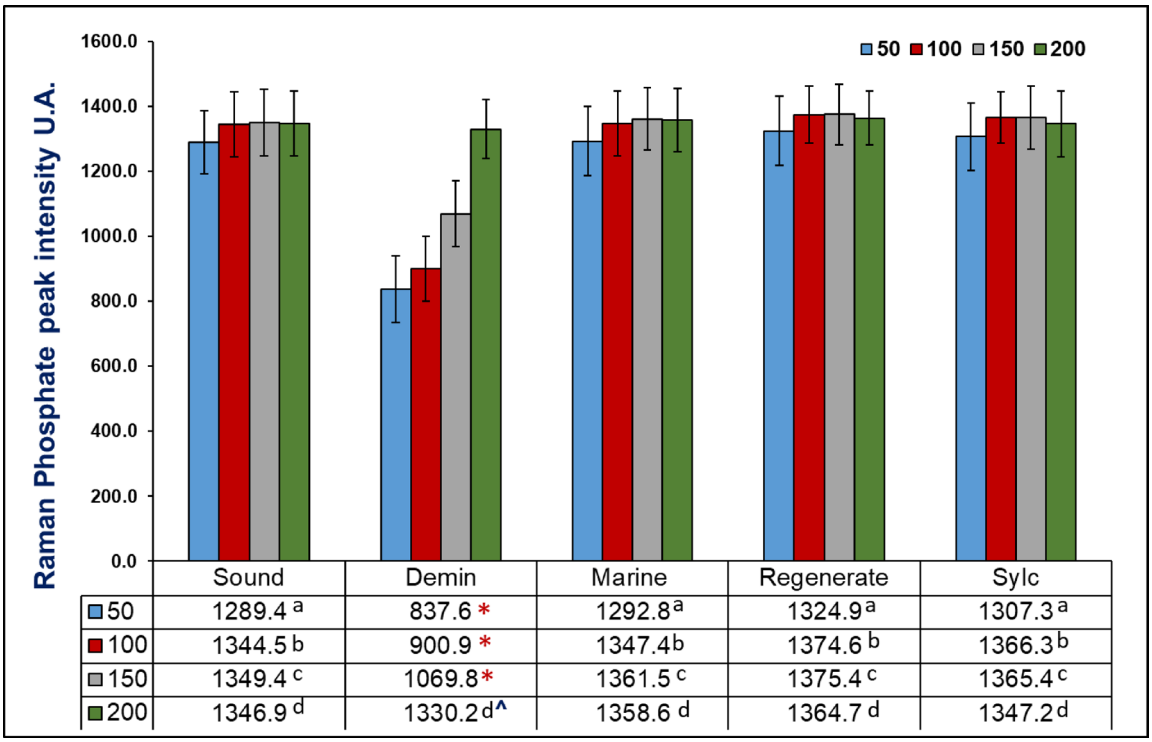

	Sound	Demin	Marine	Regenerate	Sylc
50	1289.4 [a]	837.6 *	1292.8 [a]	1324.9 [a]	1307.3 [a]
100	1344.5 [b]	900.9 *	1347.4 [b]	1374.6 [b]	1366.3 [b]
150	1349.4 [c]	1069.8 *	1361.5 [c]	1375.4 [c]	1365.4 [c]
200	1346.9 [d]	1330.2 d^	1358.6 [d]	1364.7 [d]	1347.2 [d]

Fig. 3. Raman phosphate mean intensity values (A.U.) of non-treated (sound and WSLs) and treated enamel surfaces (Marine, Regenerate, and Sylc). (*) Statistically significant differences between groups at each layer ($p < 0.001$). Similar letters indicate no significant difference between groups at each layer ($p > 0.05$). (^) Statistically significant difference for each group between layers, Multivariant ANOVA followed by Tukey's post-hoc tests (alpha level of 0.05).

Micro-Raman spectral correlation with Knoop microhardness (KHN)

The phosphate intensity values of the scanned points were plotted against their correspondent Knoop hardness numbers (KHN) as scatter logarithmic regression diagrams for all groups at different lesion depth (50–200 µm, Fig. 5). The coefficient of determination was calculated across the entire depth of enamel lesions. The highest statistically significant positive correlation was observed at the superficial layers (50 and 100 µm), $R^2 = 0.789$, 0.738, respectively (Pearson correlation, $p < 0.001$). This correlation was decreased towards the deeper layers (150 µm depth, $R^2 = 0.670$, $p < 0.001$) with a weak statistically non-significant correlation at 200 µm in all groups ($R^2 = 0.104$, $p = 0.472$). This indicates that the increase in the phosphate intensity in all groups ($p > 0.05$ between groups) was associated with an increase in microhardness up to 150 µm of the lesion depth (Fig. 5).

The morphological assessment

The sound surface (Fig. 6, A-1-4) appears smooth and homogenous associated with well-coalesced enamel rods, while the prismatic structure, the boundaries of prisms and inter-prism gaps cannot be recognized. In WSL (Fig. 6, B-1 and 2), there is a disorganized rough surface associated with higher prism exposure and higher surface porosity with the appearance of honeycomb-like structure (white arrow). Similarly in the cross-sectional view (Fig. 6, B3 and 4), the roughness, porosities, grooves, and scratches at the surface are clearly visible (blue arrow).

The surface image of Marine-treated enamel (Fig. 6, C-1 and 2) reveals rough surface with the presence of clustered aggregation of mineral-like structure covering the exposed lesion surface (white arrow head) with a reduced porosity, however, in the cross-sectional view (Fig. 6, C-3 and 4), the minerals form a compact layer covering the outer edge of the treated lesion, where the prismatic structures and inter-prism gaps were no longer distinct (blue arrow head). In contrast, the mineral precipitations in regenerate-treated surface appear (Fig. 6, D-1 and 2) as a plate-like structures with small particles scattered over the surface (yellow star) reducing the porosity of WSL. However, in the cross-section view (Fig. 6, D-3 and 4), the surface appears rougher than Marine-treated surface, and the prisms and interprism gaps were partially covered with mineral depositions along the prismatic borders (red arrow). In Sylc group, the surface appears irregular but smoother than regenerate-treated surface with a compact mineral-like layer covering the lesion surface (Fig. 6, E-1 and 2), with the evidence of small mineral deposits distributed over the treated surface (yellow star). In the cross-sectional micrographs (Fig. 6, E-3 and 4), the prisms and inter-prism gaps were masked with mineral depositions where the prismatic structures are no easily recognized (yellow arrow) restoring the defect of enamel prism after demineralization.

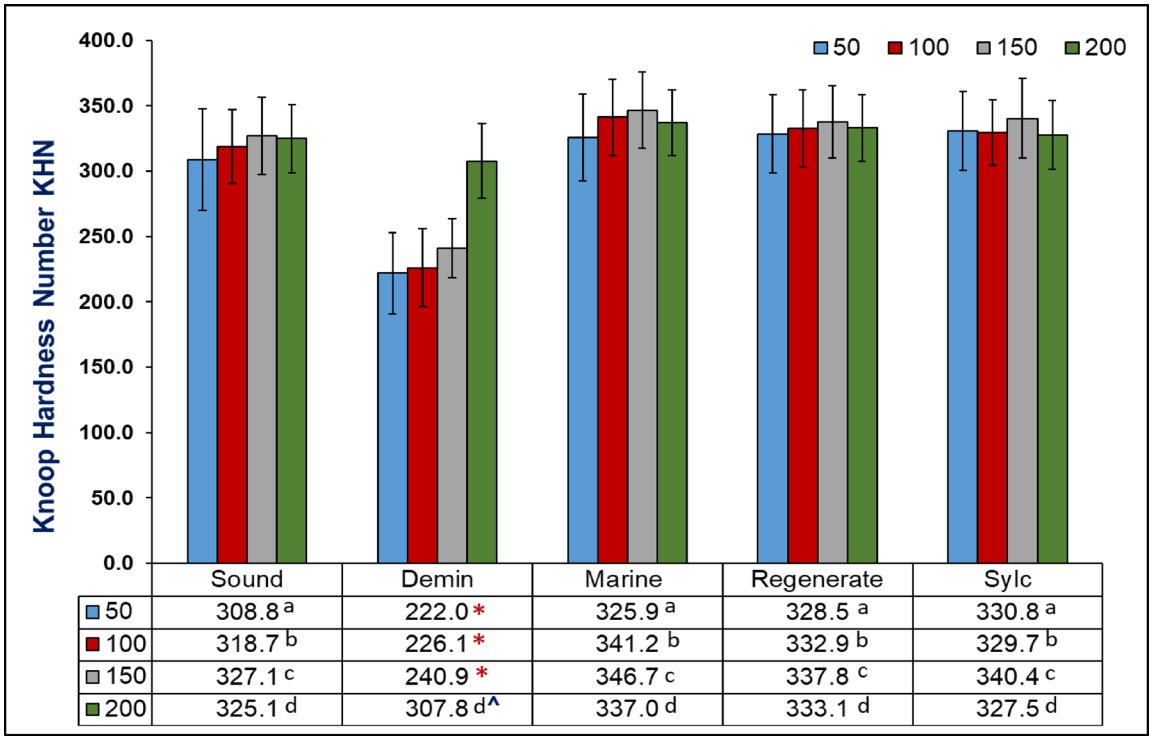

	Sound	Demin	Marine	Regenerate	Sylc
50	308.8 [a]	222.0 *	325.9 [a]	328.5 [a]	330.8 [a]
100	318.7 [b]	226.1 *	341.2 [b]	332.9 [b]	329.7 [b]
150	327.1 [c]	240.9 *	346.7 [c]	337.8 [c]	340.4 [c]
200	325.1 [d]	307.8 [d]^	337.0 [d]	333.1 [d]	327.5 [d]

Fig. 4. Knoop hardness mean values (KHN) of non-treated (sound and WSLs) and treated enamel surfaces (Marine, Regenerate, and Sylc). (*) Statistically significant differences between groups at each layer ($p < 0.001$). Similar letters indicate no significant difference between groups at each layer ($p > 0.05$). (^) Statistically significant difference for each group between layers, Multivariant ANOVA followed by Tukey's post-hoc tests (alpha level of 0.05).

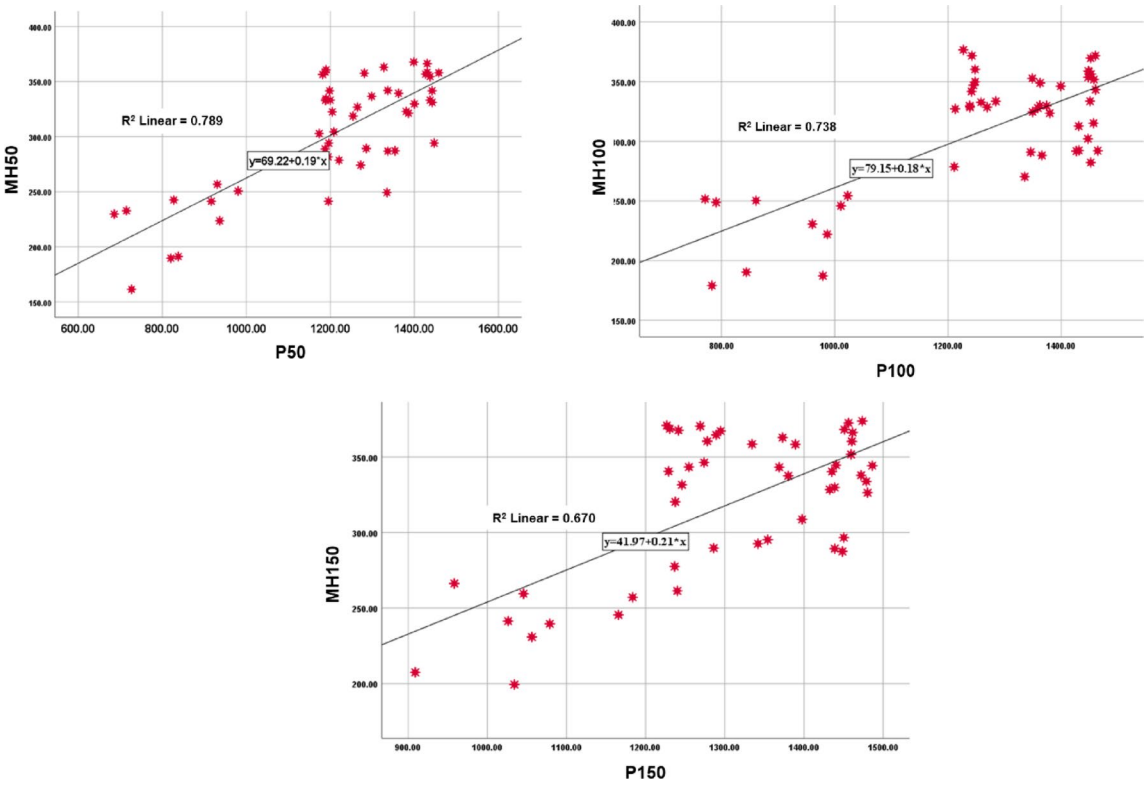

Fig. 5. The scatter plot and regression lines (R) showing the presence of a logarithmic regression positive relationship ($p < 0.001$) between phosphate intensity and the corresponding Knoop microhardness number (KHN) in all groups at three different depths (50, 100, and150 µm). The higher peak intensity values are associated with higher KHN values.

Discussion

The marine-origin collagens are biocompatible and biodegradable materials that are recently included in many dietary and pharmaceutical supplements with potential advantages in tissue engineering applications[15,30]. They possess structural and functional properties due to their unique charge distribution and affinity to self-assembled forming three-dimensional biomimetic scaffolds capable of nucleating hydroxyapatite that helps in preventing and treating dental caries[31]. Previous studies examined their effects in vitro or in animal models, with no previous study examined their effect on demineralized tooth tissues. This study hypothesized that exposure of incipient enamel lesions (WSLs) to marine collagen supplement for 28 days followed by four weeks' storage in artificial saliva can promote tissue repair in comparison to other mineralizable methods (Regenerate system, and Sylc air abrasion). The results revealed that the marine collagen can enhance the phosphate content and KHN of treated lesions as compared to WSLs up to 150 µm ($p < 0.001$), but the values were comparable to sound enamel and other treated surfaces across the lesion depth (50–200 µm, $p > 0.05$), leading to a partial rejection of the proposed hypothesis.

The secondary structure of collagen proteins was detected in the FT-IR spectrum of Marine collagen as amide I, amide II and amide III bands within the range of 1636–1661 cm^{-1}, 1549–1558 cm^{-1} and1200–1300 cm^{-1}, respectively, (Fig. 2). This finding confirms the structural integrity of the collagen protein molecules[29] as specific peptide structures with predefined secondary structures can serve as templates for the crystallization of inorganic minerals[32]. Moreover, the presence of the protein band at 1450 cm^{-1} corresponds to C-H bending modes, and the ratio of the absorption intensity of amide III to C-H bonds was close to 1.0, which is referred to the triple helical configuration of Marine collagen[33,34].

Tooth enamel is a complex mineralized tissue with a unique structural, mechanical and aesthetic properties. This is due to the high mineral contents in the form of elongated hydroxyapatite crystals arranged in a parallel fashion, with the interwoven prisms form a three-dimensional structure. These characteristics contribute to the hardness, resilience, toughness, and fracture resistance of enamel. During enamel development, matrix proteins create self-assembling supramolecular structures that regulate the disposition and morphology of hydroxyapatite crystals, and thus affect the mechanical properties of mature enamel[35].

The carious process results in progressive subsurface demineralization of enamel with mineral loss leading to mechanical failure and cavitation. Micro-Raman spectroscopy revealed a significant reduction (> 30%) in the intensity of the phosphate peak (v1 PO_4^{3-}) at 960 cm^{-1}, indicating tissue demineralization up to 150 µm depth in the WSLs, compared to sound enamel surfaces ($p < 0.001$, Fig. 3). This peak is recognized as the most robust signal in the Raman spectrum referred to the phosphate-based crystalline minerals in enamel, and deemed to be a quantitative measure for mineral loss/gain. The observed reduction in intensity signifies the dissolution of

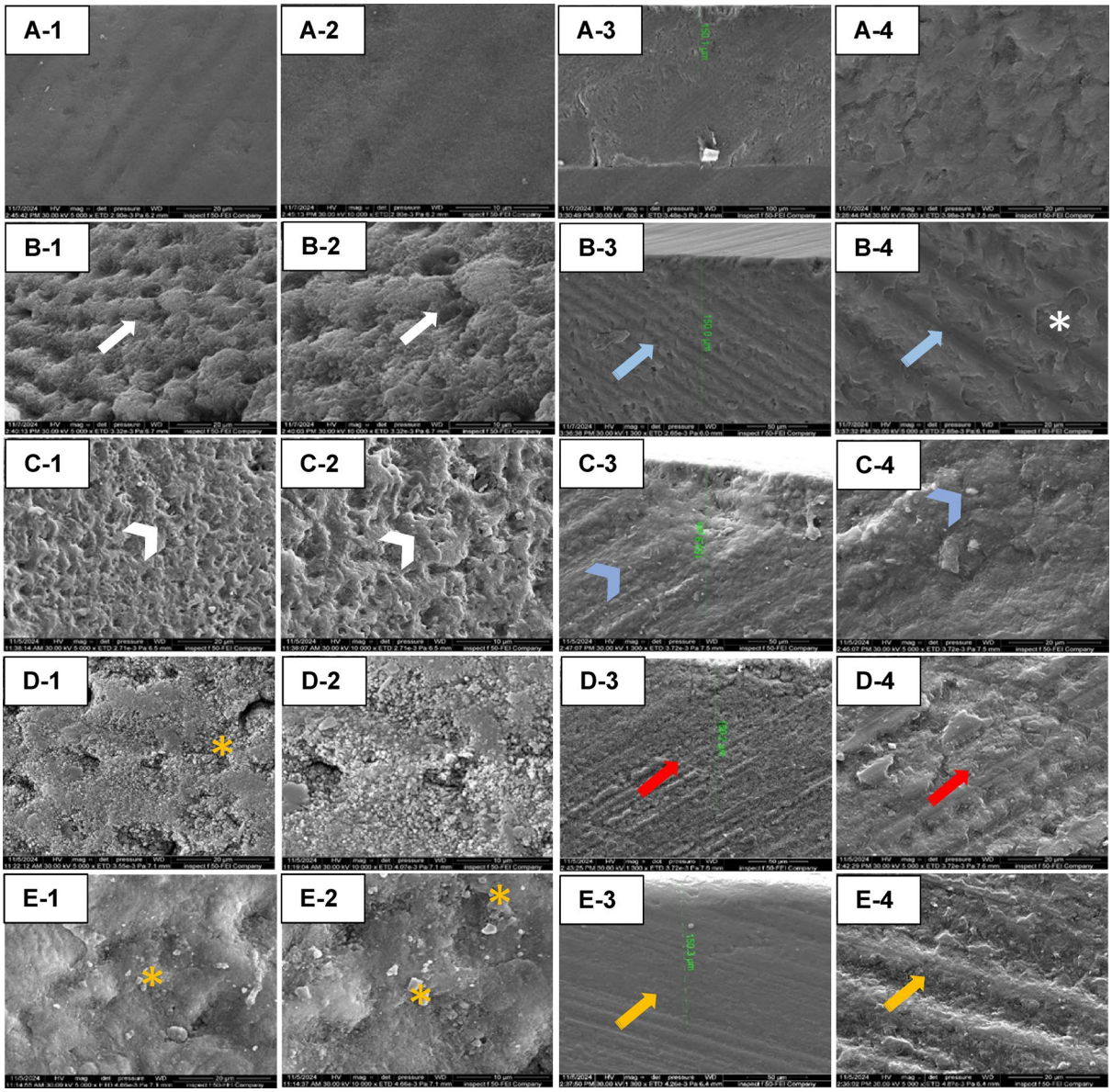

Fig. 6. Scanning electron micrographs showing the surface and cross-sectional morphology of non-treated (sound and WSL, **A** and **B**, respectively), and the treated enamel surfaces (Marine, Regenerate, and Sylc, **C**, **D**, **E**, respectively).

hydroxyapatite (HAp) crystals in enamel under acidic conditions[3,36]. Additionally, there was a notable reduction in Knoop hardness values (KHN, $p < 0.001$) up to 150 µm depth in the demineralized enamel surfaces (Fig. 4).

This lesion was produced by a bi-layer demineralization protocol using 8% MC gel buffered with a lactic acid layer (0.1 M, pH 4.6) for 21 days at 37 °C[6,18,37]. It is based on using a thick MC gel over the enamel surface to decelerate the attack of lactic acid, thus manipulating the rate of dissolution resembling natural WSLs. During immersion in the demineralization solution, hydrogen ions penetrated the enamel while calcium and phosphate ions were released, that mimics the dynamic process of caries development associated with the dissolution of HAp crystals. This significantly impacts the inter-crystalline and inter-prismatic spaces within enamel, leading to defects and cracks in the enamel surface. Scanning electron micrographs (Fig. 6: B1 and B2) support this evidence, as it shows a disorganized rough surface with higher prism exposure and porosity. In contrast, the sound surface is smooth and homogeneous (Fig. 6: A1-2), with well-coalesced enamel rods and less discernible prismatic structure (Fig. 6: A3-4). At 200 µm depth, the phosphate band intensity and Knoop hardness values equated to those of sound or treated enamel surfaces ($p > 0.05$). This observation aligns with another studys[6] that reported the depth of this lesion spans between 100 and 150 µm when measured by optical coherence tomography (OCT).

Interestingly, marine-treated surfaces recorded significantly higher mean phosphate intensity and tissue hardness values as compared to WSLs ($p > 0.001$) up to 150 µm depth, approaching those of sound enamel ($p > 0.05$, Figs. 3 and 4). This is consistent with a previous study[31] that reported a significant mineral gain in carious-like

lesions treated by self-assembled peptide for five days, suggesting the possibility of this peptide to form networks that facilitate the deposition and growth of elongated enamel-like apatite with high packing density, organized into decussating enamel rods when immersed in calcium and phosphate- containing solutions. Previous studies[38,39] affirmed the higher remineralization potential of self-assembling peptides P11-4 that support their capability to regenerate hydroxyapatite crystals by leveraging the natural remineralization properties of saliva. Moreover, it was reported[38] that self-assembled collagen could enhance the mechanical properties of enamel up to 125 µm in depth and revealed superiority over fluoride-containing agents. However, Scholz et al. (2022)[40] reported the inability of oligopeptide p11-4 to precipitate on sound enamel compared to cerium and fluoride, as the nitrogen in this peptide was not detected by energy dispersive X-ray spectroscopy (EDX). This might be due to the lack of chemical affinity or structural compatibility of the oligopeptide p11-4 to interact with sound enamel, which has a highly organized crystalline structure that is resistant to the precipitation of proteins or peptides. Moreover, the high mineralization and degree of hydrophobicity of sound enamel may reduce its interaction with hydrophilic peptides. In contrast, marine collagen is considered hydrophilic, due to the presence of hydrophilic amino acids, such as glycine, proline, and hydroxyproline. These amino acids are often used in dietary supplements that are blended with water to enhance skin health and elasticity[14]. Additionally, marine collagen is an amphoteric electrolyte with a pH-responsive function. Each collagen peptide chain contains several acidic or basic side groups, all of which can accept or donate protons. As the pH changes, these dissociable groups can become either neutral or charged within a specific pH range. This property affects calcium binding affinity, particularly on demineralized surfaces[41]. Generally, the peptides possess specific functionalities that allow them to interact more effectively with demineralized or porous enamel than with intact enamel surfaces. So, they may be more effective in remineralization processes than in adherence.

Marine-treated surfaces showed rough textures with clusters of mineral-like structures covering the exposed lesion reducing the porosity of the surface (Fig. 6: C1 and 2). The honeycomb-like structures and lacunae between enamel rods were diminished. These mineral deposits were clearly detected in the cross-sectional images (Fig. 6: C3 and C4), where a compact mineral layer enveloped the treated lesion's outer edge and prismatic structures along inter-prism gaps were obscured by mineral deposits.

The phosphate mean intensity and KHN values of marine-treated surfaces were comparable to those of Regenerate and Sylc-treated surfaces ($p > 0.05$). Although, the differences in values were statistically significant compared to WSLs up to 150 µm ($p < 0.001$), but they were comparable to untreated sound enamel surfaces across the lesion depth (50–200 µm, $p > 0.05$), leading to a partial rejection of the first hypothesis.

The regenerate-treated surfaces exhibited highest phosphate peak intensity among groups throughout the entire lesion depth (50–200 µm, Fig. 3); however, the difference was statistically not significant ($p > 0.05$). This efficacy arises from the ability of calcium silicate and phosphate to form mineral complexes that can precipitate and seal enamel lesions, as illustrated in Fig. 6: D1 and D2. The calcium ions can replace the hydrogen ions (H^+) in the surrounding environment forming silanol compounds (Si-OH). As the pH increases near negatively charged surfaces, Si-O support the precipitation of mineral deposits[16,36]. Furthermore, the salivary phosphate groups (PO_4^{3-}) attract calcium ions through silanol group, resulting in a calcium phosphate CaP-enriched layer vital for enamel remineralization. This finding aligns with a clinical study[36] confirming the deposition of minerals on bovine inserts after four weeks of brushing with a toothpaste containing calcium silicate and sodium phosphate salts. Moreover, another study[17] reported higher Raman phosphate peak intensity and tissue hardness in enamel surfaces treated by regenerate system before and after pH-cycling. Additionally, the presence of calcium and phosphate salts may amplify fluoride release, enhancing enamel's re-hardening capacity and promoting remineralization. This supports the higher microhardness values of this treatment group in comparison to WSLs at depths up to 150 µm ($p > 0.001$). This concurs with other studies[42,43] that noted improved hardness values in demineralized enamel surfaces following the application of Remin Pro and MI Paste Plus, which contain calcium, phosphate, and fluoride. The acidic fluoride can interact with calcium, resulting in the deposition of CaF_2-like complexes on enamel surfaces at low pH. These complexes serve as a reservoir for fluoride ions, which adsorb onto partially demineralized crystals, facilitating tissue remineralization[44].

In the current study, mineral precipitations appeared as plate-like structures (Fig. 6: D1 and D2) with small minerals scattered across the surface reducing the porosity in treated WSLs. However, in the cross-sectional view (Fig. 6: D3 and D4), the surface appears rough compared to marine-treated, and the prisms and inter-prism gaps are partially covered by mineral deposits along the prismatic borders.

Although Sylc -treated surfaces exhibited higher phosphate content compared to untreated WSLs ($p > 0.001$) up to 150 µm depth, the difference compared to sound and other treated groups was statistically insignificant ($p > 0.05$) across the entire depth of lesions. This suggests greater availability of phosphate ions resulting from the remineralization therapy. Previous studies[18,30,45,46] reported that Sylc-treated surfaces manifested higher microhardness values than untreated lesions. This improvement likely reflects mineral deposition within lesions, a result of the bioactive glass 45S5 (BAG) which forms hydroxy-carbonate apatite (HCA) structures. Upon contact with saliva, active ingredients (calcium, phosphate, and silicate ions) from BAG dissolve at the glass surface, exchanging with those in the solution. This interaction elevates the interfacial pH, leading to the precipitation of a silica-rich layer that serves as a matrix template for amorphous calcium phosphate formation, which later crystallizes into HCA[45]. The bioactive properties of BAG and the precipitation process at lesion surfaces are evident in SEM images (Fig. 6: E1-4), revealing a compact mineral-like layer covering lesion surfaces and small mineral deposits dispersed on BAG-treated surfaces. These minerals cover the prisms and inter-prism gaps, in the cross-sectional micrographs (Fig. 6: D3 and D4) restoring the prism integrity after demineralization.

In agreement with previous studies[17,47] a positive correlation was observed between the chemical composition and mechanical gradient up to 150 µm depth (Pearson correlation, $p < 0.001$). The strongest correlations had occurred at superficial layers (50 and 100 µm, $R^2 = 0.789$, 0.738, respectively), indicating that the increase in phosphate intensity in all groups was associated with higher microhardness values. However, at the deepest layer

(200 µm), there was a weak insignificant correlation observed in all groups ($R^2 = 0.104$, $p = 0.472$, Fig. 5); thus, the hypothesis was partly rejected.

The translation of biomimetic remineralization strategy necessitates further clinical studies as most in-vitro studies rely on the immersion of specimens in remineralization solutions containing peptide analogues, which is difficult to achieve clinically. Furthermore, the artificial saliva is composed of inorganic ions only, with no consideration for the effect of salivary proteins, pellicle and plaque on mineralization inhibition. Moreover, there is possibility of structural variations in enamel due to the exposure to different oral conditions among specimens. The inclusion of fluoride as a positive control in this study is strongly advised. However, the use of other systems that have a beneficial impact on enamel remineralization are also worthy of consideration as positive controls. While the study indicated that marine collagen consumption has positive effects, factors such as the severity of lesions, oral hygiene routines, dietary habits, and a person's overall oral health could also influence the clinical outcome. Therefore, this treatment should not be seen as a substitute for professional cleanings and fluoride applications.

Conclusions

The findings of the present study affirm the positive impact of marine collagen supplement in repairing enamel white spot lesions, especially when compared to two remineralization methods. This was observed by the considerable increase in the phosphate intensity and microhardness values in marine-treated surfaces compared to untreated WSLs, approaching those of Regenerate and Sylc-treated surfaces, and sound enamel throughout the entire depth of the lesions (50–200 µm). These results highlight the potential ability of this approach to repair demineralized enamel surfaces, allowing the development of a biomimetic protective layer that enhances the integrity and morphology of demineralized enamel surfaces.

Data availability

The data that support the findings of the current study are available from corresponding author upon reasonable request.

Received: 22 December 2024; Accepted: 1 August 2025
Published online: 11 August 2025

References

1. Tang, S., Dong, Z., Ke, X., Luo, J. & Li, J. Advances in biomineralization-inspired materials for hard tissue repair. *Int. J. Oral Sci.* **13**, 42. https://doi.org/10.1038/s41368-021-00147-z (2021).
2. Vivaldi-Rodrigues, G., Demito, C. F., Bowman, S. J. & Ramos, A. L. The effectiveness of a fluoride varnish in preventing the development of white spot lesions. *World J. Ortho.* **7**, 2 (2006). https://pubmed.ncbi.nlm.nih.gov/16779972/
3. Yetkiner, E., Wegehaupt, F., Wiegand, A., Attin, R. & Attin, T. Colour improvement and stability of white spot lesions following infiltration, micro-abrasion, or fluoride treatments in vitro. *Eur. J. Ortho.* **36**, 5. https://doi.org/10.1093/ejo/cjt095 (2014).
4. Al- Mamoori, R. M. H. & Al Haidar, A. H. M. Effect of resin infiltration and microabrasion on the microhardness of the artificial white spot lesions (an in vitro study). *J. Baghdad Coll. Dent.* **34**, 1. https://doi.org/10.26477/jbcd.v34i1.3091 (2022).
5. Patil, N., Choudhari, S., Kulkarni, S. & Joshi, S. R. Comparative evaluation of remineralizing potential of three agents on artificially demineralized human enamel: an: in vitro: study. *J. Conserv. Dent. Endod.* **16**, 2. https://doi.org/10.4103/0972-0707.108185 (2013).
6. Al-Taee, L., Banerjee, A. & Deb, S. In-vitro adhesive and interfacial analysis of a phosphorylated resin polyalkenoate cement bonded to dental hard tissues. *J. Dent.* **118**, 104050. https://doi.org/10.1016/j.jdent.2022.104050 (2022).
7. Pandya, M. & Diekwisch, T. G. H. Enamel biomimetics-fiction or future of dentistry. *Int. J. Oral Sci.* **11**, 8. https://doi.org/10.1038/s41368-018-0038-6 (2019).
8. Alkilzy, M., Qadri, G., Splieth, C. H. & Santamaría, R. M. Biomimetic enamel regeneration using Self-Assembling peptide P_{11}-4. *Biomimetics* **8**, 290. https://doi.org/10.3390/biomimetics8030290 (2023).
9. Wang, Q. Q. et al. Biomimetic oligopeptide formed enamel-like tissue and dentin tubule occlusion via mineralization for dentin hypersensitivity treatment. *J. Appl. Biomater. Funct. Mater.* **19**, 22808000211005384. https://doi.org/10.1177/22808000211005384 (2021).
10. Kind, L. et al. Biomimetic remineralization of carious lesions by self-assembling peptide. *J. Dent. Res.* **96**, 790–797. https://doi.org/10.1177/0022034517698419 (2017).
11. Coppola, D. et al. Marine collagen from alternative and sustainable sources: extraction, processing and applications. *Mar. Drugs.* **18**, 214. https://doi.org/10.3390/md18040214 (2020).
12. Cho, W. et al. Low-molecular-weight fish collagen peptide (valine-glycine-proline-hydroxyproline-glycine-proline-alanine-glycine) prevents osteoarthritis symptoms in chondrocytes and monoiodoacetate-injected rats. *Mar. Drugs.* **21**, 608. https://doi.org/10.3390/md21120608 (2023).
13. Dai, M., Sui, B., Xue, Y., Liu, X. & Sun, J. Cartilage repair in degenerative osteoarthritis mediated by squid type II collagen via Immunomodulating activation of M2 macrophages, inhibiting apoptosis and hypertrophy of chondrocytes. *Biomaterials* **180**, 91–103. https://doi.org/10.1016/j.biomaterials.2018.07.011(2018).
14. Farooq, S. et al. A review on marine collagen: sources, extraction methods, colloids properties, and food applications. *Collagen Leather.* **6**, 11. https://doi.org/10.1186/s42825-024-00152-y (2024).
15. Kim, S. C., Heo, S. Y., Oh, G. W., Yi, M. & Jung, W. K. A 3D-Printed polycaprolactone/marine collagen scaffold reinforced with carbonated hydroxyapatite from fish bones for bone regeneration. *Mar. Drugs.* **20**, 344. https://doi.org/10.3390/md20060344 (2022).
16. Parker, A. S. et al. Measurement of the efficacy of calcium silicate for the protection and repair of dental enamel. *J. Dent.* **42** https://doi.org/10.1016/S0300-5712(14)50004-8 (2014). S21-S29.
17. Shubbar, M., Addie, A. & Al-Taee, L. The effect of a bioactive oral system and CO2 laser on enamel susceptibility to acid challenge. *Diagnostics* **13**, 1087. https://doi.org/10.3390/diagnostics13061087 (2023).
18. Milly, H., Festy, F., Watson, T. F., Thompson, I. & Banerjee, A. Enamel white spot lesions can remineralise using bio-active glass and polyacrylic acid-modified bio-active glass powders. *J. Dent.* **42**, 158–166. https://doi.org/10.1016/j.jdent.2013.11.012 (2014).
19. Taha, A. A., Fleming, P. S., Hill, R. G. & Patel, M. P. Enamel remineralization with novel bioactive glass air abrasion. *J. Dent. Res.* **97**, 1438–1444. https://doi.org/10.1177/0022034518792048 (2018).
20. Chabuk, M. M. & Al-Shamma, A. M. Surface roughness and microhardness of enamel white spot lesions treated with different treatment methods. *Heliyon* **9**, e18283. https://doi.org/10.1016/j.heliyon.2023.e18283 (2023).

21. Al-Obaidi, R., Salehi, H., Desoutter, A., Tassery, H. & Cuisinier, F. Formation and assessment of enamel subsurface lesions in vitro. *J. Oral Sci.* **61**, 454–458. https://doi.org/10.2334/josnusd.18-0174 (2019).
22. Lippert, F. Effect of enamel caries lesion baseline severity on fluoride Dose-Response. *Int. J. Dent.* **1**, 4321925. https://doi.org/10.1155/2017/4321925 (2017).
23. Amaechi, B. T. & Van Loveren, C. Fluorides and non-fluoride remineralization systems. Toothpastes Monogr. *Oral Sci. Basel Karger*. **23**, 15–26. https://doi.org/10.1159/000350458 (2013).
24. Lippert, F., Al-Shareefi, S., Addie, A. & Al-Taee, L. Al-Shareefi, S., Addie, A. & Al-Taee, L. Biochemical and mechanical analysis of occlusal and proximal carious lesions. *Diagnostics*. **12**, 2944. (2022). https://doi.org/10.3390/diagnostics12122944
25. Hamdi, K., Hamama, H. H., Motawea, A., Fawzy, A. & Mahmoud, S. H. Remineralization of early enamel lesions with a novel prepared tricalcium silicate paste. *Sci. Rep.* **12**, 9926. https://doi.org/10.1038/s41598-022-13608-0 (2022).
26. Faul, F., Erdfelder, E., Buchner, A. & Lang, A. G. Statistical power analyses using G*Power 3.1: tests for correlation and regression analyses. *Behav. Res. Methods*. **41**, 1149–1160. https://doi.org/10.3758/BRM.41.4.1149 (2009).
27. El-Wassefy, N. A. The effect of plasma treatment and bioglass paste on enamel white spot lesions. *Saudi J. Dent. Res.* **8**, 58–66. https://doi.org/10.1016/j.sjdr.2016.10.001 (2017).
28. de Marsillac, M. D. W. S. & de Vieira, S. Assessment of artificial caries lesions through scanning electron microscopy and cross-sectional microhardness test. *Indian J. Dent. Res.* **24**, 249–254. https://doi.org/10.4103/0970-9290.116699 (2013).
29. Sripriya, R. & Kumar, R. A novel enzymatic method for Preparation and characterization of collagen film from swim bladder of fish Rohu (Labeo rohita). *Food Sci. Nutr.* **6**, 1468–1478. https://doi.org/10.4236/fns.2015.615151 (2015).
30. Rigogliuso, S., Campora, S., Notarbartolo, M. & Ghersi, G. Recovery of bioactive compounds from marine organisms: focus on the future perspectives for pharmacological, biomedical and regenerative medicine applications of marine collagen. *Molecules* **28**, 1152. https://doi.org/10.3390/molecules28031152 (2023).
31. Kirkham, J. et al. Self-assembling peptide scaffolds promote enamel remineralization. *J. Dent. Res.* **86**, 426–430. https://doi.org/10.1177/154405910708600507 (2007).
32. Alkilzy, M., Santamaria, R. M., Schmoeckel, J. & Splieth, C. H. Treatment of carious lesions using self-assembling peptides. *Adv. Dent. Res.* **29**, 42–47. https://doi.org/10.1177/0022034517737025 (2018).
33. Al-Sagheer, R. M., Addie, A. J. & Al-Taee, L. A. An in vitro assessment of the residual dentin after using three minimally invasive caries removal techniques. *Sci. Rep.* **14**, 7087. https://doi.org/10.1038/s41598-024-57745-0 (2024).
34. Al-Badri, H., Al-Taee, L. A., Banerjee, A. & Al-Shammaree, S. A. An in-vitro evaluation of residual dentin retained after using novel enzymatic-based chemomechanical caries removal agents. *Sci. Rep.* **14**, 19223. https://doi.org/10.1038/s41598-024-69763-z (2024).
35. Kirkham, J. et al. Physico-chemical properties of crystal surfaces in matrix–mineral interactions during mammalian biomineralisation. *Curr. Opin. Colloid Interface Sci.* **7**, 124–132. https://doi.org/10.1016/S1359-0294(02)00017-1 (2002).
36. Sun, Y. et al. Mode of action studies on the formation of enamel minerals from a novel toothpaste containing calcium silicate and sodium phosphate salts. *J. Dent.* **42**, S30–S38. https://doi.org/10.1016/S0300-5712(14)50005-X (2014).
37. White, D. J., Chen, W. C. & Nancollas, G. H. Kinetic and physical aspects of enamel remineralization- a constant composition study. *Caries Res.* **22**, 11–19. https://doi.org/10.1159/000261077 (1988).
38. Schmidlin, P., Zobrist, K., Attin, T. & Wegehaupt, F. In vitro re-hardening of artificial enamel caries lesions using enamel matrix proteins or self-assembling peptides. *J. Appl. Oral Sci.* **24**, 31–36. https://doi.org/10.1590/1678-775720150352 (2016).
39. Üstün, N. & Aktören, O. Analysis of efficacy of the self-assembling peptide-based remineralization agent on artificial enamel lesions. *Microsc Res. Tech.* **82**, 1065–1072. https://doi.org/10.1002/jemt.23254 (2019).
40. Scholz, K. J. et al. Surface accumulation of cerium, self-assembling peptide, and fluoride on sound bovine enamel. *Bioengineering* **9**, 760. https://doi.org/10.3390/bioengineering9120760 (2022).
41. Wu, K., Li, Y. & Chen, J. Effect of pH on the structure, functional properties and rheological properties of collagen from Greenfin horse-faced filefish (Thamnaconus septentrionalis) skin. *Mar. Drugs*. **22**, 45. https://doi.org/10.3390/md22010045 (2024).
42. Esfahani, K. S., Mazaheri, R. & Pishevar, L. Effects of treatment with various remineralizing agents on the microhardness of demineralized enamel surface. *J. Dent. Res. Dent. Clin. Dent. Prospects*. **9**, 239–245. https://doi.org/10.15171/joddd.2015.043 (2015).
43. Almarsomy, D. H., Al-Khayat, F. A. & Al-Taee, L. A. The preventive/therapeutic effect of CO2 laser and MI paste Plus® on intact and demineralized enamel against Streptococcus mutans (In vitro Study). *Heliyon* **9**, e20310. https://doi.org/10.1016/j.heliyon.2023.e20310 (2023).
44. Scholz, K. J. et al. EDX-analysis of fluoride precipitation on human enamel. *Sci. Rep.* **9**, 13442. https://doi.org/10.1038/s41598-019-49742-5 (2019).
45. Soares, R., De Ataide, I. D. N., Fernandes, M. & Lambor, R. Assessment of enamel remineralisation after treatment with four different remineralising agents: a scanning electron microscopy (SEM) study. *J. Clin. Diagn. Res.* **11**, ZC136–ZC141. https://doi.org/10.7860/JCDR/2017/23594.9758 (2017).
46. Rahee, S. S. & Jehad, R. H. Comparing the effectiveness of using three different re-mineralizing pastes on remineralisation of artificially induced white spot lesion. *J. Baghdad Coll. Dent.* **35**, 35–45. https://doi.org/10.26477/jbcd.v35i4.3512 (2023).
47. Magalhães, A. C. et al. Comparison of cross-sectional hardness and transverse microradiography of artificial carious enamel lesions induced by different demineralising solutions and gels. *Caries Res.* **43**, 474–483. https://doi.org/10.1159/000264685 (2009).

Acknowledgements

The authors acknowledged the College of Dentistry, University of Baghdad, Ministry of Higher Education and Scientific Research, Baghdad/Iraq, for providing the facilities and the ultimate support to accomplish this study.

Author contributions

H.J.-C: methodology, investigation, data curation, writing-original draft preparation. L.A.-T.: conceptualization, methodology, writing-review and editing, supervision.

Declarations

Competing interests

The authors declare no competing interests.

Additional information

Correspondence and requests for materials should be addressed to L.A.A.-T.